Gyroscopically enhanced vertical axis pendulum for wave energy conversion

Masturi, Lurohman M.; Hendrikse, Hayo; Jarquin Laguna, Antonio J.; Metrikine, Andrei V.

Gyroscopically enhanced vertical axis pendulum for wave energy conversion

Lurohman M. Masturi, Hayo Hendrikse, Antonio J. Laguna, and Andrei V. Metrikine

Abstract—The vertical axis pendulum is a type of point absorber device which can absorb wave energy from a width exceeding the physical width of the device. Mechanical power is harvested from the rotation of the pendulum, in which the pivot point is directly connected to the generator. In this paper, a new concept of the vertical axis pendulum device is proposed by adding a spinning flywheel to create a gyroscopic effect with the aim to enhance the motions of the pendulum. In the vertical axis of the pendulum, the reaction torque from the power take off (PTO) is included as a linear function of the pendulum rotation velocity to model the mechanical power conversion into electrical power. The initial spinning velocity of the flywheel is used as the parameter to obtain the maximum energy in the PTO. To demonstrate the effect of adding a flywheel to the pendulum system, two models are simulated and compared, i.e. a classical vertical axis pendulum and a 'gyroscopic-pendulum'. The results of the comparison are presented in terms of the pendulum motions and the PTO converted power.

Keywords—Coupled pendulum, gyroscopic effect, wave energy converter.

I. Introduction

W AVE energy application can be a solution to fulfil the electricity demand for the more remote islands, in which case the access to electricity and a grid might be limited or non-existent. This type of energy is environmentally friendly, available around the clock and can be installed in every coastal area. Several prototypes of Wave Energy Converters (WECs) have

been shown to successfully produce electricity [1][2]. The efficiency of these devices compared to other energy converting devices remains a significant challenge for the development of WECs.

A. Existing point absorber type of wave energy converters

For harvesting energy from waves, several types of converting devices have been implemented in the past. Salter, who is known as the founding father of wave energy, proposed the nodding duck in 1974. The duck can be considered as the first wave energy device studied in Europe [3]. The duck is asymmetric, floating and slack moored and positioned orthogonally with the incoming wave. Due to its asymmetric geometry, the duck starts to nod and create a rocking motion. Another device that utilizes the asymmetric floater shape to convert wave energy is Searev (Système Électrique Autonome de Récupération d'Énergie des Vagues) [4]. The center of gravity of the device is off-centered by enclosing a heavy horizontal axis cylinder. The system behaves mechanically, like a pendulum rotating relative to the hull. The rotating motion is used as mechanical power to activate power take-off followed by conversion into electricity.

In the development of the duck, Salter used a series of 'ducks' in an array, which is classified as a 'terminator'. Each device is positioned differently with respect to the incoming wave which causes the devices to rotate with a phase difference [5]. A gyro canister is installed in each device to extract the energy from the combination of a spinning disk of the gyro and rocking motion of the duck [6]. The concept of a gyro is also used in ISWEC (Inertial Sea Wave Energy Converter) [1]. This device utilizes the gyroscopic-effect to convert electricity from the pitch motion of the floater. In combination with the spinning flywheel and the rocking motions in the pitch direction, it creates a torque along the PTO's shaft. This torque drives the electrical generator to extract energy from the system.

The device described in [3] has a pendulum which is free to rotate inside the floating body. The energy is extracted from the wave induced rotation of the pendulum. Numerical modelling and experimental validation are performed. The application of the device is used as a self-powered buoy for navigation or as a data buoy. Another device that uses a pendulum rotating in the vertical axis is the penguin WEC, established by
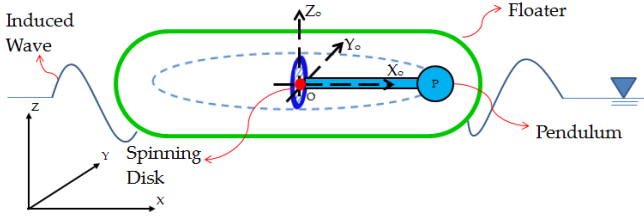
Fig. 1. Concept drawing of the wave energy converter including the spinning disk, pendulum, and a simple representation of the floating body.

Wello [2]. The Wello floater has an asymmetric shape and mimics the flaps of a penguin. The waves excite a the hull motions which drives the mass to rotate around the generator shaft which produces electricity directly. The device has been successfully tested since 2012 and grid-connected at EMEC site in Orkney, Scotland. Recently, Wello Oy has been agreed to provide 10 MW Wello Penguin to Nusa Penida Island in Bali, Indonesia through Gapura Energi Utama (GEU), an Indonesian infrastructure construction company. It will be the largest wave energy park in the world [9].

B. Gyroscopic-pendulum device

In this paper, a preliminary analysis of a new technical concept for marine energy generation inside a floating module is presented. The concept is to convert marine energy into mechanical power, using the rotational motion of a vertical horizontal pendulum driven by wave actions and gyroscopic effect from a controlled spinning disk. This system is referred to as the 'gyroscopic-pendulum'. A concept drawing for the wave energy converter is provided in Fig. 1.

The gyroscopic-pendulum device is a modification of the classic vertical axis pendulum device with the additional of a spinning disk connected in the pendulum axis. The spinning disk and the torque originating from the pendulum weight, together create a gyroscopic effect which drive the pendulum to rotate around the Z_o-axis. This phenomenon is called precession. The mechanical power is generated from the rotational motion of the pendulum. The optimum power is produced when the frequency of the rotating pendulum meets with the frequency of the floater motions induced by the hydrodynamic forces on the floater. The waves induced floater motions and the pendulum rotations which are enhanced by the gyroscopic effect (the precession) from the flywheel drives the pendulum to rotate faster. The advantage of combining a spinning disk with a pendulum is found in the ability to tune the pendulum rotation in order to reduce the losses associated to start-up and stopping as well as to provide control of its motions in different sea states.

II. MODEL DESCRIPTION

The gyroscopic-pendulum model that consists of the vertical axis pendulum and the flywheel is fixed to the floater and free to rotate around the vertical axis such that the motions of the floater in roll and pitch are equal to the motions of the pendulum in the same directions. It is noted here that the hydrodynamic coupling that comes from wave actions on the floater is not discussed in this paper.

C. Pendulum velocity vector

The device itself consists of two rotating components; a spinning disk rotating around the pendulum-axis and a pendulum rotating around the Z_o-axis at the pivot Point O. In this paper, the centre of rotation of the floater is assumed to coincide with Point O. By using this configuration, the pendulum can be modelled as a point mass (m_p) at a distance l from the pivot point. The generator is assumed to be positioned in the same axis as the rotating pendulum and electricity is produced by the relative rotation of the pendulum and the floater rotation around the Z_o-axis (i.e. yaw). The pendulum rotation is further coupled with the rotations of the floater around the X_o-axis (i.e. roll) and the floater rotation around the Y_o-axis (i.e. pitch).

It is convenient to describe the components orientation relative to the global coordinate system [10]. Here, the global coordinate system is denoted by XYZ and $X_oY_oZ_o$ are used for the local coordinate system. The pendulum position in the local coordinate system is defined as the distance from the origin of local coordinate system (O) to the centre of mass of the pendulum (P).

$$\overrightarrow{OP} = \begin{bmatrix} l \\ 0 \\ 0 \end{bmatrix} \tag{1}$$

The concept of the Eulerian angles is one of the most used kinematic representation of rotating devices [11]. Here, a rotation matrix $\boldsymbol{J}$ is used to defined the pendulum position as a function of an Euler angle. The matrix $\boldsymbol{J}$ is composed of three rotation matrices: the pendulum rotation matrix ($\boldsymbol{C}_{Z_o,\psi}$), pitch matrix ($\boldsymbol{C}_{Y_o,\theta_f}$), and roll matrix ($\boldsymbol{C}_{X_o,\varphi_f}$). Matrix multiplication rules are applied in the rotation matrix, $\boldsymbol{J^T}$, with the pendulum position vector $\overrightarrow{OP}$ to describe the pendulum position vector after rotation in the global coordinate system ($\vec{r}_p$).

$$\vec{r}_p = \boldsymbol{J^T} \cdot \overrightarrow{OP} \tag{2}$$

$$\vec{r}_p = \begin{bmatrix} c\theta_f \, c\psi \, l \\ (s\psi \, c\varphi_f + c\psi \, s\theta_f \, s\varphi_f)l \\ (s\psi \, s\varphi_f - c\psi \, s\theta_f \, c\varphi_f)l \end{bmatrix} \tag{3}$$

Where, $s \cdot = sin(\cdot)$, and $c \cdot = cos(\cdot)$. In order to define the angle of pendulum rotation (ψ), pitch (θ_f) and roll (φ_f), a snap-shot of the pendulum mass position with respect to the global coordinate system is made. Fig.2 shows the description of pendulum in global coordinate system as a function of pitch and roll. The continuous
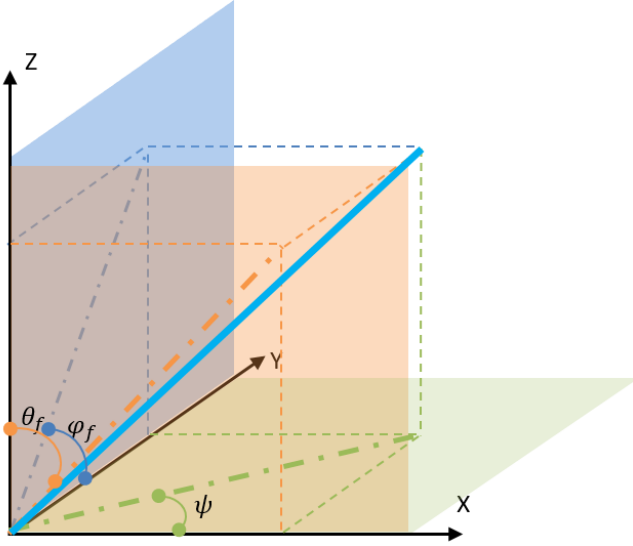
Fig. 2. Description of pendulum position in the global coordinate system.

thick line is a snap-shot of the pendulum position in an arbitrary plane. Dashed thick lines with dots represent the projection line of the pendulum in the plane. ψ is an angle between the *X*-axis of the global coordinate system and the pendulum projection on the *X-Y* plane. φ_f is an angle between the *Y*-axis of the global coordinate system and the pendulum projection on the *Y-Z* plane. θ_f is an angle between the *Z*-axis of the global coordinate system and the pendulum projection on the *X-Z* plane. Furthermore, the velocity vector of the pendulum $(\dot{\vec{r}}_p)$ is calculated as the time derivative of $\vec{r}_p$:

$$\dot{\vec{r}}_p = \frac{d\vec{r}_p}{dt} \tag{4}$$

D. Angular velocity vector

The angular velocity vector of the device is defined by the orientation of the local coordinate system with respect to the global coordinate system [11]. In addition to the spinning disk, the angular velocity of the pendulum is determined by the same rotation order of the rotation matrix (*J*). In total, the gyroscopic-pendulum velocity vector $(\vec{\omega}_p)$ is consisting of the pendulum motions $(\dot{\psi})$, the spinning disk $(\dot{\varphi})$, the pitch motions $(\dot{\theta}_f)$ and the roll motions $(\dot{\varphi}_f)$.

$$\vec{\omega}_p = \begin{bmatrix} \dot{\varphi} \\ 0 \\ 0 \end{bmatrix} + \begin{bmatrix} \dot{\varphi}_f \\ 0 \\ 0 \end{bmatrix} + C_{x,\varphi_f} \begin{bmatrix} 0 \\ \dot{\theta}_f \\ 0 \end{bmatrix} + C_{x,\varphi_f} C_{y,\theta_f} \begin{bmatrix} 0 \\ 0 \\ \dot{\psi} \end{bmatrix} \tag{5}$$

$$\vec{\omega}_d = \begin{bmatrix} \dot{\varphi} \\ 0 \\ 0 \end{bmatrix} + \begin{bmatrix} 0 \\ \dot{\theta}_f \\ 0 \end{bmatrix} + C_{y,\theta_f} \begin{bmatrix} 0 \\ 0 \\ \dot{\psi} \end{bmatrix} \tag{6}$$

The angular velocity vector of the flywheel $(\vec{\omega}_d)$ contains pendulum motions $(\dot{\psi})$, the spinning disk $(\dot{\varphi})$, and the pitch motions $(\dot{\theta}_f)$. The spinning disk is free to rotate around the pendulum axis such that its angular velocity is decoupled from the roll motion.

E. Moment of inertia

Based on the device configuration in Fig. 1, the inertia tensor of the pendulum (I_p) is a function of time. Whereas the disk has constant moment of inertia (I_d) since the disk is always rotating in the pendulum axis at Point O. For the point mass pendulum, the simplified angular momentum (Λ) formulation can be used to compute the inertia tensor.

$$\Lambda = \left(\vec{r}_p \times \left(\vec{\omega}_s \times \vec{r}_p \right) \right) m_p = I_p \, \vec{\omega}_s \tag{7}$$

III. MATHEMATICAL MODEL

F. Equations of motion

A mathematical model is established to couple the two degrees of freedom of the pendulum system with the roll and pitch motions of the floater. The disk and pendulum are described as a rigid body. In this paper, the Lagrange formalism is chosen as the method for developing the dynamic model [12]. Application of the Lagrangian formulation requires the energy for each component to be described. The kinetic energy is calculated from the translation and rotation of the pendulum, and rotation of the flywheel, while the potential energy is only calculated for the pendulum since the flywheel is located at the origin of the local coordinate system.

The pendulum produces kinetic energy from both translation and rotation (T_p). The potential energy of the pendulum is calculated from the vertical distance of the pendulum mass position with respect to the origin of the local coordinate system. The vertical distance of pendulum is calculated by projecting the pendulum position vector on Zo $(\vec{r}_p \cdot \vec{k})$ where $\vec{k}$ is a unit vector of the *Zo*-axis. In addition, the potential energy of spring in the pitch degree of freedom is considered to model restoring forces on the floater. The stiffness coefficient in the pitch direction is given by k_{θ_f}.

The disk has only kinetic energy (T_d) due to rotation of its own centre of gravity at Point O.

$$L = T - V \tag{8}$$

$$T_p = \frac{1}{2} \dot{\vec{r}}_p^T m_p \dot{\vec{r}}_p + \frac{1}{2} \vec{\omega}_p^T I_p \vec{\omega}_p \tag{9}$$

$$V = m_p g \left(\vec{r}_p \cdot \vec{k} \right) + \frac{1}{2} k_{\theta_f} \theta_f^2 \tag{10}$$
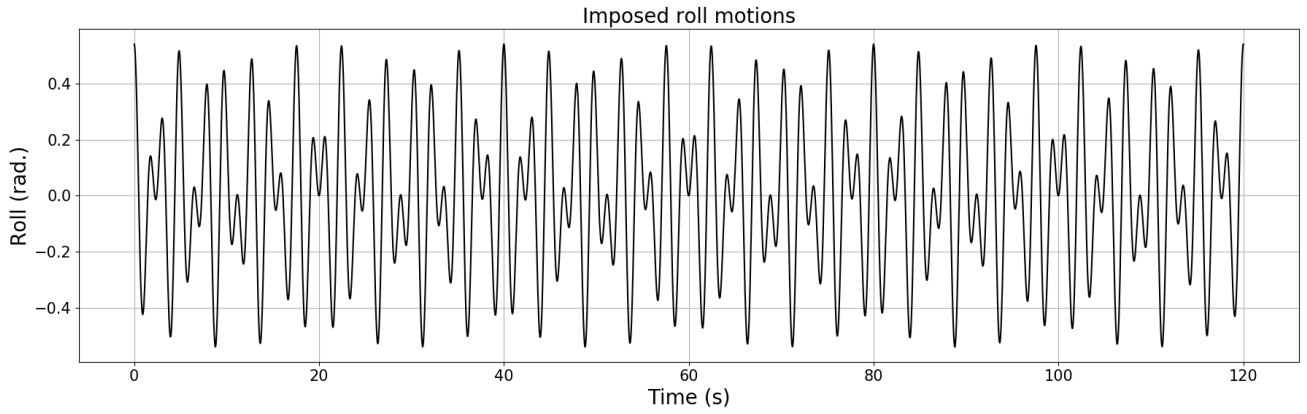
Imposed roll motions

Fig. 3. Imposed motions in roll direction.

$$T_d = \frac{1}{2} \vec{\omega}_d{}^T I_d \, \vec{\omega}_d \tag{11}$$

Where g is the gravitational acceleration. Four coupled equations of motion (EOM) are established based on (12) which together describe the dynamic behaviour of the gyroscopic-pendulum system.

$$\frac{d}{dt}\left(\frac{\partial L}{\partial \dot{q}_j}\right) - \frac{\partial L}{\partial q_j} + \frac{\partial F}{\partial \dot{q}_j} = 0 \tag{12}$$

Subscript 'j' refers to degree of freedom of the system such as pendulum rotation, disk rotation, roll and pitch motions. q_j and $\dot{q}_j$ indicate the position and time derivative of the position. Damping coefficient is introduced by using Rayleigh dissipation function (F).

$$F = \sum_j \frac{1}{2} c_j \, \dot{q}_j{}^2 \tag{13}$$

Since the floater motions induce the rotation of the vertical axis pendulum models, the EOM has a potential energy component as shown in (10). Therefore, the damping (c_{θ_f}) and stiffness (k_{θ_f}) coefficients in the pitch direction are added to obtain the reasonable results on the numerical model solutions. In both models, the classical pendulum and the gyroscopic-pendulum, the same coefficients are applied.

G. PTO model

An electrical generator is assumed connected directly on the pendulum axis to capture the torque from pendulum rotation which provides mechanical power. The mechanical power transmits into a generator torque that converts into electrical power. This configuration of a power take off (PTO) system will be used to convert

TABLE I
INPUT FOR MODELS

Symbol	Description	Quantity [Unit]
m_p	Pendulum mass	30 [kg]
I_d	Disk mass moment of inertia[a]	5 [kg·m²]
l	Length of pendulum	1 [m]
k_{θ_f}	Stiffness coefficient in the pitch direction.	257.5 [kg·m²·s⁻²]
c_{θ_f}	Damping coefficient in the pitch direction	0.203 [kg·m²·s⁻¹]
c_p	PTO damping of the pendulum	0.106 [kg·m²·s⁻¹]
c_d	Viscous damping on the disk	0.005 [kg·m²·s⁻¹]
ω_d	Initial angular velocity of the disk[a]	0.542 [rad/s]

[a]Applied only for the gyroscopic-pendulum model.

mechanical power into electrical power. The actual system has not yet been studied, but the most common model for PTO is a damper system [1]. The generator torque (T_{PTO}) is absorbed from the rotation of pendulum by the damper. Furthermore, the mechanical power output (P_{exp}) on the PTO can be calculated as a function of the generator torque and angular velocity of the pendulum in which the PTO is assumed as an ideal system (lossless).

$$T_{PTO} = c_s \dot{\psi} \tag{14}$$

$$P_{exp} = T_{PTO} \dot{\psi} \tag{15}$$

Where c_s is the viscous damping of the damper system used to represent the PTO.
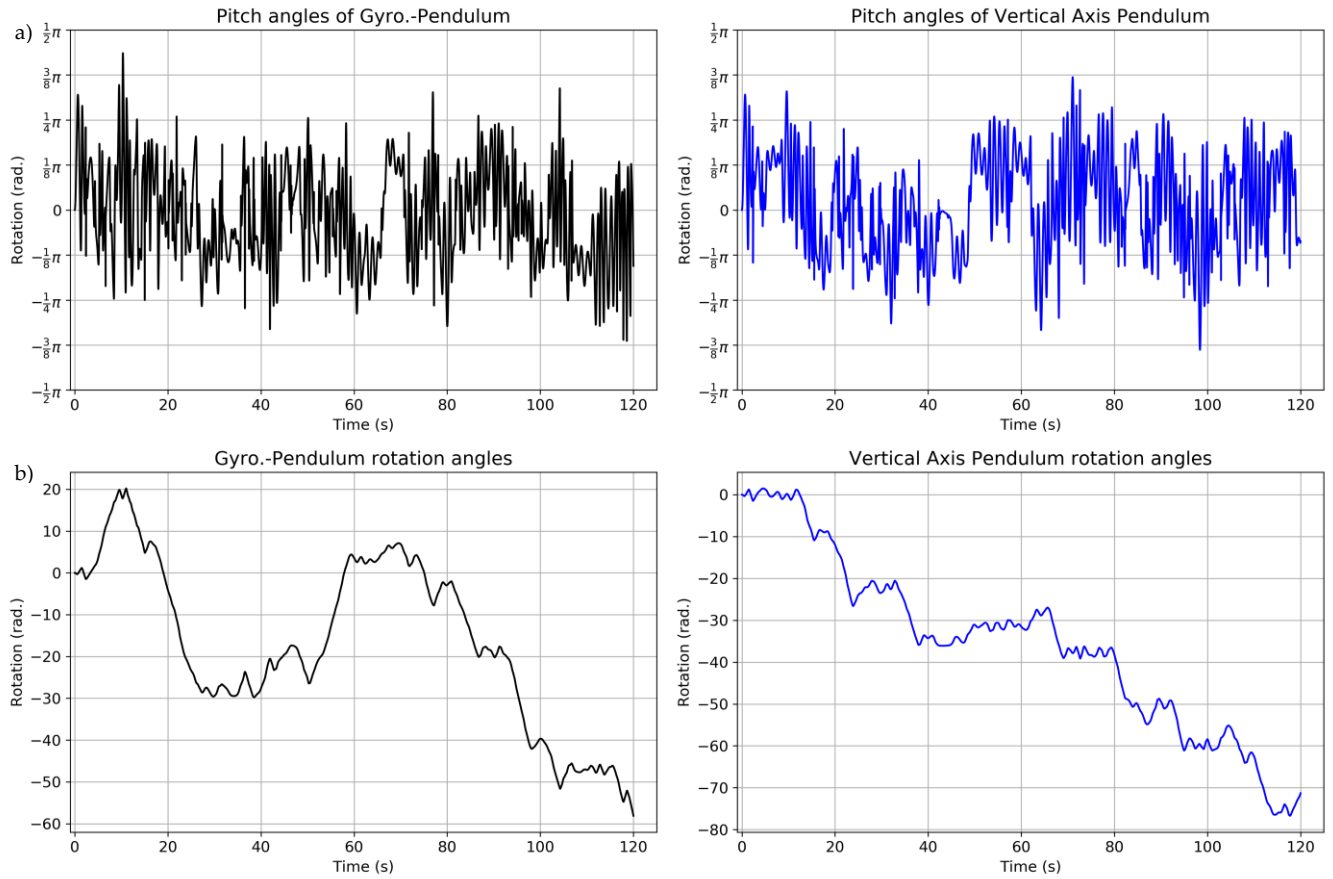
IV. MODEL COMPARISON

Fig. 4. Time plot pendulum position comparison between gyroscopic-pendulum and vertical axis pendulum.

The effect of the spinning disk on the velocity of the vertical axis pendulum is studied by comparing the gyroscopic-pendulum and the classical vertical axis pendulum. A model for the vertical axis pendulum is established using the same approached discussed in Section III, but removing the DOF corresponding the angular velocity of the spinning disk from the equations of motion.

The equations of motion are solved numerically in the time domain using general solvers for initial value problem of ordinary differential equations (ODE) in Python using the ODEINT package [13]. The same input values for both models are introduced except for the disk properties (I_d) which are only applicable to the gyroscopic-pendulum model. For the comparison presented here, the motions in the roll direction are imposed as shown in Fig. 3. The imposed roll motion is used to mimic in a simplified manner irregularity of the floater motions induced by wave loading. Table I shows other input parameters that are used in the model for the comparison.

For the gyroscopic-pendulum model, an angular velocity of the spinning disk is given as initial condition at t = 0 as shown in Table I. The determination of the kinetic energy associated to this velocity is further discussed in the Results section.

V. RESULTS

Time domain analysis using ODEINT solver is used to study the dynamic behaviour of both pendulum models. An example of the pendulum positions as a function of time is shown in Fig. 4. As shown in Fig. 3, the imposed motions that are introduced in the roll direction can be also described as the pendulum positions in roll angles.

The imposed motions that are introduced are sufficient to rotate the pendulum around the vertical axis. The counter clockwise direction of pendulum rotation is indicated by a positive value. The differences in pendulum rotation between the two models is caused by introduction of the flywheel in the gyroscopic-pendulum model. Energy is introduced in the flywheel for its initial rotation. In order to define the energy input on the flywheel, a parametric model of the gyroscopic-pendulum has been developed and investigated. In this model, a range of values for the initial energy input has been used as an input and the value for this study was chosen based on the maximum absorbed energy by the gyroscopic-pendulum over a 30 seconds interval. Fig. 5 shows the optimum initial velocity of the flywheel (i.e. 0.542 rad/s) in order to achieve maximum absorbed energy.
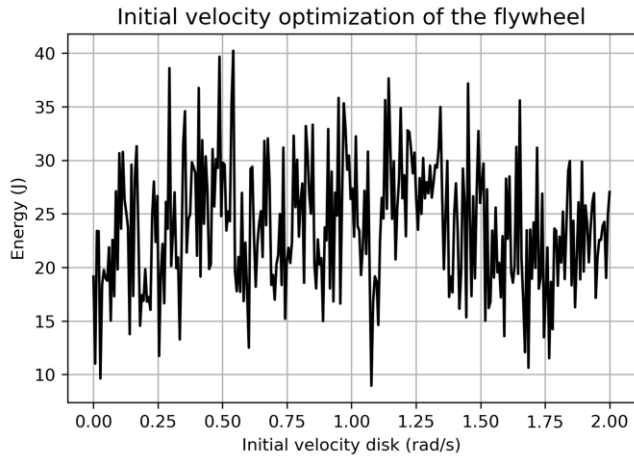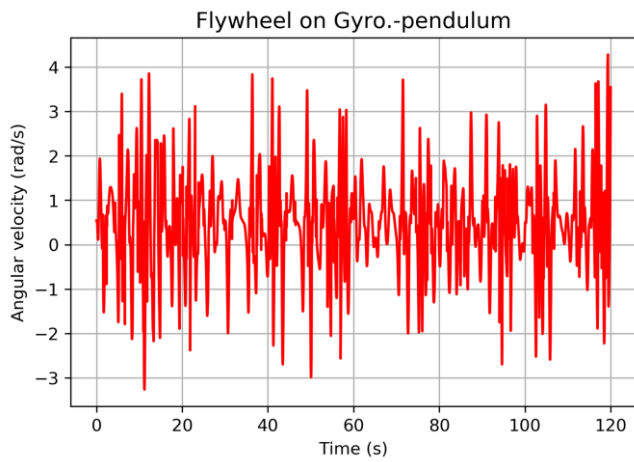
Fig. 5. Energy input study for the flywheel

Fig. 6. Time plot of rotation and angular velocity of the flywheel
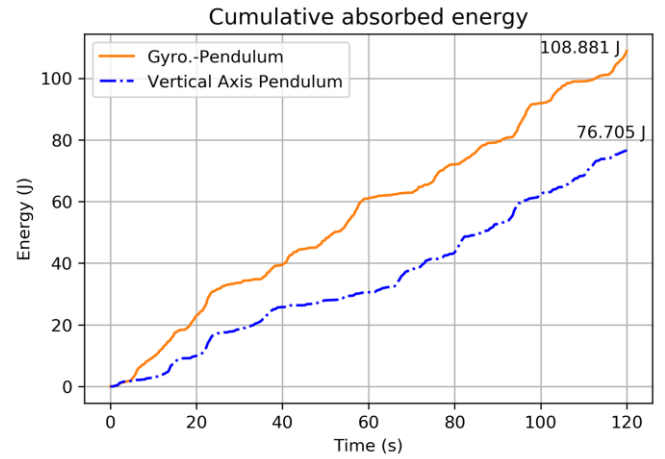

Fig. 7. Absorbed energy from the pendulum rotation comparison between the gyroscopic-pendulum model and the vertical axis pendulum model.

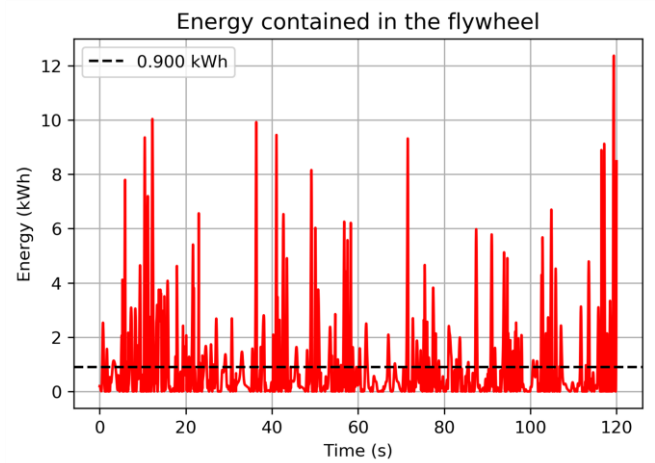Fig. 8. Stored energy in the flywheel.

The energy input required in the flywheel is the kinetic energy that is used to spin the disk. The kinetic energy input on the disk (E_d) is calculated by multiplying the inertia of the disk (I_d) with the square of the initial velocity required for the disk (ω_d).

$$E_d = \frac{1}{2} I_d \, \omega_d{}^2 \tag{16}$$

The Initial velocity on the flywheel creates a precession on the pendulum due to the gyroscopic effect. In Fig. 6, the flywheel angular velocity is presented. It can be seen that the flywheel is not rotating with a constant velocity. This is a consequence from the coupling between the flywheel with the pendulum rotations and the pitch motions.

The effects of coupling between the flywheel and the pendulum are also observed in the gyroscopic-pendulum model which causes the distinct pendulum rotation as shown in Fig. 4b.

The objective of the device is to enhance the angular velocity of the vertical axis pendulum by adding the gyroscopic effect. It is shown here as an example that by using a suitable magnitude for the rotation of the flywheel, the gyroscopic-pendulum produces more absorbed energy than the vertical axis pendulum as shown in Fig. 7. The cumulative absorbed energy of the pendulums is presented as a time integration of the mechanical power output that is absorbed by the PTO during the duration of the simulation.

Since the gyroscopic pendulum model requires the energy input to rotate the flywheel, the total cumulative absorbed energy for this model should be reduced by the energy input (E_d). If the energy input required to initially spin the disk is around 0.734 J (Calculated based on (16)) then the net energy absorbed by the gyroscopic pendulum is 108.147 J which is a factor 1.41 larger than the energy absorbed by the vertical axis pendulum (i.e. 76.705 J).

As shown in (5), the angular velocity of the disk is coupled with the pitch and pendulum motions. If the disk is situated in the almost vacuum chamber to minimize the friction loss, the flywheel can be used as an energy storage. In this paper, a very small damping coefficient (c_d) is used to model the air resistance in the flywheel chamber. The energy storage in the flywheel chamber can be used to generate precession on the pendulum rotations and maximize the pendulum rotations in case there are only small waves available. In Fig. 8, dashed thick lines indicates the average energy contained in the flywheel in kWh. The investigation regarding the storage of energy

and its use to rotate the pendulum will be studied in the future.

VI. CONCLUSION

Based on a preliminary numerical simulation it is shown that gyroscopic effect introduced in the gyroscopic-pendulum allows to enhance the absorbed energy compared to the classical vertical axis pendulum.

Further study of the gyroscopic-pendulum is planned, namely verification and validation of the numerical model in dry and wet experiments, development of a control system for the spinning disk, and ultimately developing power take-off (PTO) model to optimize the power production of the system.

REFERENCES

[1] G. Bracco, "ISWEC: a gyroscopic wave energy converter," Ph.D. dissertation, Politecnico di Torino, Italy, 2010.

[2] M. Korppi, "Wello Penguin WEC," in Bilbao Marine Energy Week, Bilbao, Spain, 2014.

[3] S. H. Salter. "Wave power," *Journal of Nature*, vol. 249, pp. 720-724, 1974.

[4] A. Clément, A. Babarit, J. C. Gilloteaux, C. Josset, G. Duclos, "The searev wave energy converter," in 6th European Wave and Tidal Energy Conference, 2005, pp. 81-90.

[5] S. H. Salter. "Recent progress on ducks ," presented at *the IEE PROC*, vol. 127, no. 5, 1980.

[6] S. H. Salter, "The use of gyros as a reference frame in wave energy converters," presented at *The 2nd International Symposium on Wave Energy Utilization*, pp. 99-115, 1982.

[7] S. H. Salter. "Power conversion systems for ducks," presented at *the IEE 'Future Energy Concept' conference*, 1979.

[8] J. G. Bretl, "A time domain model for wave induced motions coupled to energy extraction," Ph.D. dissertation, The University of Michigan, U.S.A, 2009.

[9] H. Paakkinen, "Wello is supplying a 10 MW wave energy park to Bali," Dec. 2018. [Online]. Available: https://wello.eu/2017/12/28/wello-supplying-10-mw-wave-energy-park-bali/

[10] P. Nicola et al, "Wave tank testing of a pendulum wave energy converter 1:12 scale model," *International Journal of Applied Mechanics,* vol. 9, no. 2, pp. 1750024-1–1750024-30, 2017.

[11] T. I. Fossen, "Nonlinear modelling and control of underwater vehicles," Ph.D. dissertation, Norwegian Institute of Technology, Norway, 1987.

[12] T. R. Kurfess, "Lagrangian Dynamics," in *Robotics and Automation Handbook*. CRC Press LLC, USA, 2005, ch. 5, pp. 1-21.

[13] W. Weckesser, "scipy.integrate.odepack.py," May. 2018. [Online]. Available: https://github.com/scipy/scipy/blob/v1.2.1/scipy/integrate/odepack.py#L28-L259

[14] J. Falnes, Ocean Waves and Oscillating Systems: Linear Interactions Including Wave-Energy Extraction. Cambridge: Cambridge University Press, 2002.